Studying the corrosion resistance and hydrolytic degradation of an epoxy coating containing ZnO nanoparticles

B. Ramezanzadeh, M.M. Attar*

Department of Polymer Engineering and Color Technology, Amirkabir University of Technology, P.O. Box 15875-4413, Tehran, Iran

ARTICLE INFO

ABSTRACT

Epoxy nanocomposites containing different contents of Nano-ZnO particles were prepared. The nanocomposites were exposed to 3.5 wt% NaCl solution up to 60 days. Mechanical properties of the nanocomposites (before and after exposure to NaCl solution) were studied by dynamic mechanical thermal analysis (DMTA) and nano-indentation techniques. Fourier transform infrared spectroscopy (FTIR) was utilized to investigate hydrolytic degradation of coatings. Corrosion resistance of the composites was studied by an electrochemical impedance spectroscopy (EIS). Results showed that blank sample was severely deteriorated after exposure to corrosive electrolyte. Corrosion resistance of the epoxy coating was significantly improved using nanoparticles. The cross-linking density and indentation hardness of the blank sample were significantly decreased after exposure to corrosive electrolyte. Results showed that nanoparticles could significantly improve coating resistance against hydrolytic degradation. Results revealed that decrease in cross-linking density and indentation hardness of the epoxy coatings containing 3.5 and 5 wt% nanoparticles were not significant. Decrease in adhesion loss was also obtained using nanoparticles.

1. Introduction

Organic coatings have been widely used to protect metal bodies from corrosion. It has been shown that organic coatings can significantly improve corrosion resistance of the metal bodied [1–4]. Different parameters such as ionic resistance and cross-linking density of coatings can influence their barrier performance. Increase in cross-linking density and ionic resistance may cause decrease in rate of electrolyte permeation into the coating matrix. However, decrease in cross-linking density and barrier properties of coatings can be seen after exposure to corrosive electrolyte. Hydrolytic degradation can occur during coating exposure to corrosive electrolyte. Coating degradation can result in a decrease in coating cross-linking density. Decrease in cross-linking density may also lead to holes creation. Increase in number and size of holes can be seen at long immersion times. Holes are conductive pathways for electrolyte diffusion into the coating matrix. Oxygen and water molecules can easily reach to coating/metal interface through holes. Therefore, they can significantly reduce corrosion resistance and increase adhesion loss of the coating [5–10].

Different methods have been utilized to evaluate coatings degradation after exposure to corrosive electrolytes. It has been

shown that FTIR and EIS are useful techniques to investigate hydrolytic degradation of coatings [11–18,3,19–25]. Hydrolytic degradation of coatings can be accurately studied by a FTIR technique. EIS is a non-destructive technique with high capability of revealing the first signs of coating degradation (before creation of any visual microscopic defects). Coating degradation can be also studied by investigating electrolyte diffusion into the coating matrix. Thermo-gravimetric analysis (TGA) [20,21], EIS and differential scanning calorimetry (DSC) have been extensively used to evaluate electrolyte diffusion into the coating matrix [22]. It has been shown that capacitance measurement is the most favorite method of monitoring coating degradation. Mansfeld et al. [16] used EIS to evaluate organic coatings degradation in exposure to corrosive electrolytes. Oliveira and Ferreira [2] ranked organic paints with respect to their tendency to degradation in 3% NaCl solution. Szociński et al. [23] used five-electrode system (with a split micro-reference electrode) to investigate blister creation on the organic paints which were exposed to corrosive electrolyte [23].

Attempts have been carried out to improve coating resistance against hydrolytic degradation. Anticorrosive pigments i.e. chromate, phosphate and micro sized metallic pigments have been utilized to improve corrosion resistance of the organic paints [26,27]. It has been shown that organic/inorganic pigments can significantly improve corrosion resistance of the organic paints. However, these pigments cannot improve coatings resistance against hydrolytic degradation at long immersion times [9,28]. It has been shown that nanoparticles can significantly improve

* Corresponding author. Tel.: +98 21 64542404; fax: +98 21 66468243.
E-mail address: attar@aut.ac.ir (M.M. Attar).

coating resistance against corrosion and hydrolytic degradation [29–32]. Zhang et al. [28] showed that Nano-TiO$_2$ particles can significantly improve corrosion resistance of the epoxy coating. Dhoke and Khanna [29,30] revealed that nano sized ZnO particles can effectively improve corrosion resistance of the alkyd based coatings. It has been shown that Nano-ZnO is a non-toxic nanoparticle. Therefore, environmentally friendly coatings can be produced using these nanoparticles.

In this study, it has been aimed to investigate the effects of ZnO nanoparticles on the hydrolytic degradation and corrosion resistance of an epoxy-polyamide coating.

2. Experimental

2.1. Sample preparation

ZnO nanoparticles were added to an epoxy/polyamide coating at different loadings. To this end, pre-dispersed ZnO nanoparticles (BYK-3842) were prepared from BYK Co. The average size and solid content of the nanoparticles were 40 nm and 40% respectively. Epoxy resin (Araldite G27 7071X75) with solid content, epoxy value and density of 74–76%, 0.14–0.16 Eq/100 g and 1.08 g cm^{-3} respectively was prepared from Saman Co. Nanoparticles were added to epoxy resin at weight ratios of 2, 3.5, 5 and 6.5 wt%. Nanoparticles were then dispersed in epoxy resin using a high shear mixer (2000 rpm). The mixing time was about 20 min. Stoichiometric values of polyamide curing agent were added to the nanocomposites. BYK-306 (as a leveling agent) and Efka-2025 (as defoaumer) were added to coatings in order to improve their application properties.

Corrosion resistance of the nanocomposites was studied on St-37 type steel sheets. The steel sheets (5 cm × 10 cm × 0.2 cm) were prepared from Foolad Mobarakeh Co. The elemental composition of the steel samples was studied by an energy dispersive spectroscopy (EDS) (Table 1).

Table 1
The elemental composition of the St-37 mild steel.

Weight (%)	Elemental analysis of St-37 steel sheet						
	Al	S	P	Mn	Si	C	Fe
	0.04	0.	0.05	0.32	0.34	0.19	99.01

The surface of steel sheets was carefully cleaned from mill scale and other contaminations before paint application. The mill scale layer on the steel sheets was completely removed using a magnetic polisher (2000 rpm). Samples were then degreased using a commercial acetone solvent. Finally, samples were rinsed in distilled water and dried in an oven at 40 °C.

Nanocomposites were applied over the cleaned St-37 sheets and glass plates by a film applicator. Samples were then cured at 140 °C for 30 min. The free films of the nanocomposites were prepared from glass painted plates. The dry thickness of dried coatings was about 50 ± 5 μm.

2.2. Sample characterization

Epoxy nanocomposites were exposed to 3.5 wt% NaCl solution for 60 days. The surface morphology of the nanocomposites (before and after exposure to corrosive electrolyte) was studied by a Canon type digital camera and a Leica DMR optical Microscope.

Mechanical properties of the nanocomposites (before and after exposure to corrosive electrolyte) were studied by a Tritec 2000 DMTA. The test was carried out at frequency, temperature and heating rate of 1 Hz, −30 °C to 160 °C and 5 °C min^{-1} respectively. The viscoelastic properties of the coatings were studied before and after exposure to corrosive electrolyte. To this end, a Hysitron Triboscope type nanoindenter (with tip morphology of Berkovich) was used. The test was carried out at progressive force range of 0–250 mN during 60 s. FTIR (Equinox-55) was used to investigate hydrolytic degradation of the composites.
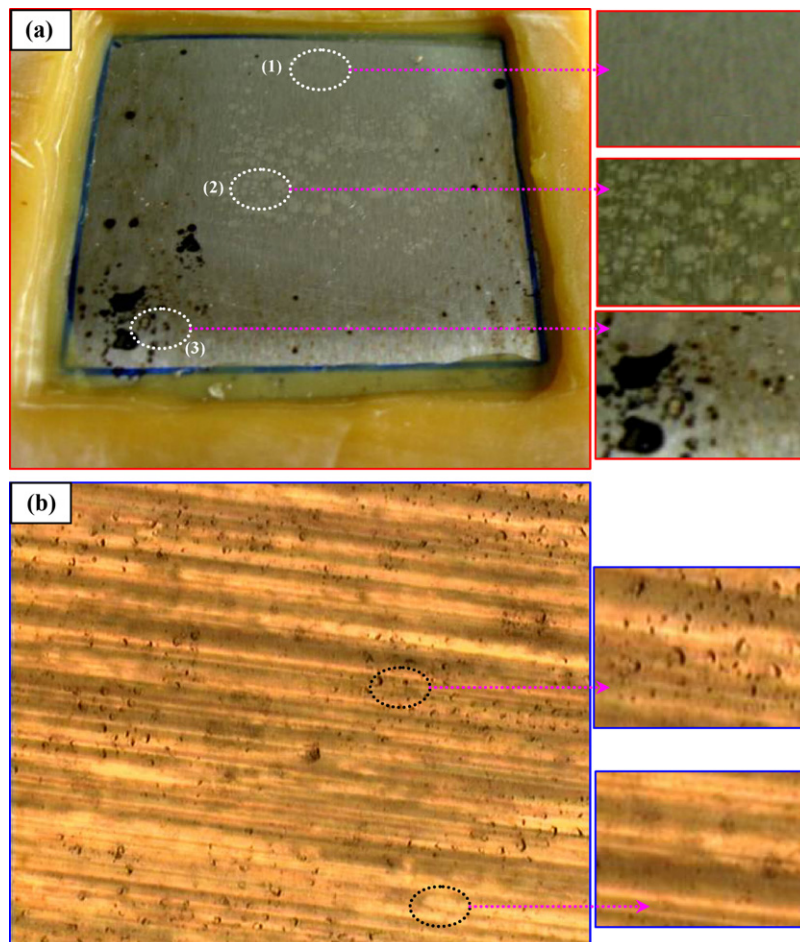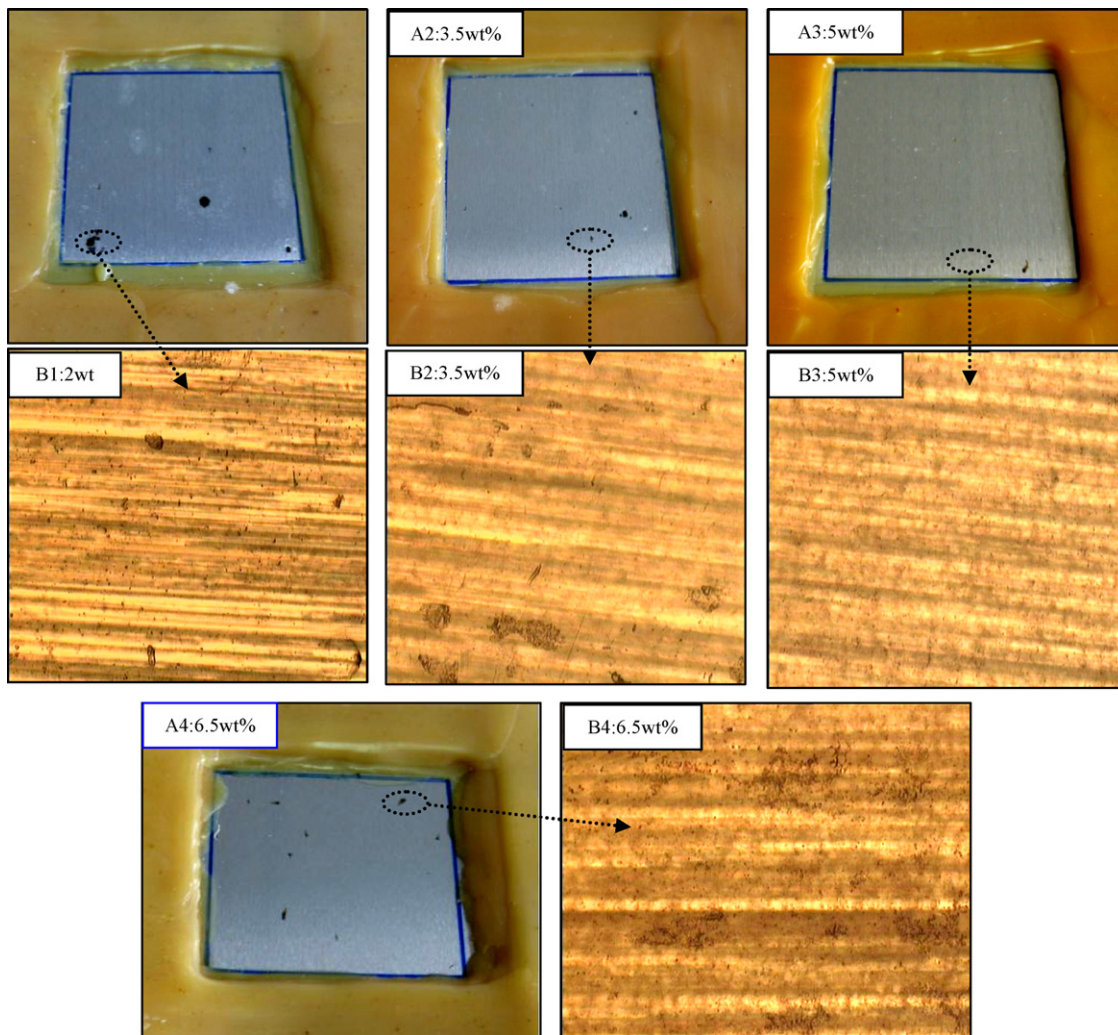

Fig. 1. Digital photograph (a) and optical micrograph (b) of the blank epoxy coating exposed to 3.5 wt% NaCl solution up to 60 days; (1) unaffected part (2) blister creation (3) corrosion products creation.

Table 2
The values of cross-linking density (ν_e), loss peak height and width, nano hardness (H) and indentation depth at maximum load (D_{max}).

Sample	Parameter				
	ν_e (mol cm^{-3})	Loss peak width (°C)	Loss peak height	H (GPa)	D_{max} (nm)
Before exposure	0.0011 ± 0.00005	11 ± 0.5	1.10 ± 0.03	0.18 ± 0.011	205 ± 3.0
After exposure	0.0003 ± 0.00002	16 ± 1.0	0.95 ± 0.05	0.13 ± 0.02	230 ± 8.0

Fig. 2. Digital photographs (A1) to (A4) and optical micrographs (B1) to (B4) of the epoxy nanocomposites exposed to 3.5 wt% NaCl solution up to 60 days.

Corrosion resistance of the nanocomposites was studied by an AUTOLAB G1 type EIS. The perturbation and frequency range of measurements were ±10 mV and 10 kHz–10 mHz respectively. The electrochemical system was including platinum electrode (auxiliary electrode), saturated Ag/AgCl electrode (reference electrode) and metal sheet (working electrode). The experiment was carried out on 9 cm^2 area of each coating at different immersion times. The adhesion strength of the coatings was determined by a Posi pull-off adhesion tester (DEFELSKO). The elemental composition of the steel sample was studied by a MV2300 type scanning electron microscope (SEM). All experiments were carried out on three replicas of each sample. In this way, the reproducibility of measurements was studied.

3. Results and discussion

3.1. Nanoparticles dispersion evaluation

It is well known that nanoparticles dispersion can significantly influence coating properties. Nano-ZnO particles dispersion in epoxy coating matrix was studied by a UV–visible and an atomic force microscope (AFM) in previous works [33,34]. It was shown

that nanoparticles (at 2 and 3.5 wt%) did not significantly change the optical transparency of the epoxy coating at wavelength region of visible light. It is well known that particles larger 100 nm can reduce coating transparency at visible light wavelength region. However, significant decrease in coating transparency was seen at 6.5 wt%. The same results were observed in AFM micrographs. These results all revealed that nanoparticles were appropriately dispersed (particle size < 100 nm) in epoxy coating matrix at 2 and 3.5 wt%. On the other hand, particles aggregation (particle size > 100 nm) was observed at 6.5 wt%.

3.2. Coating appearance after exposure to corrosive electrolyte

Epoxy nanocomposites were exposed to NaCl solution (3.5 wt%) up to 60 days. The optical micrographs of the blank epoxy coating are shown in Fig. 1.

Table 3
The values of loss peak width and indentation depth at maximum load (D_{max}).

Sample	Parameter			
	Loss peak width (°C)		D_{max} (nm)	
	Before exposure to electrolyte	After exposure to electrolyte	Before exposure to electrolyte	Before exposure to electrolyte
2 wt%	12.30 ± 0.1	18.70 ± 0.25	199 ± 3	225 ± 6
3.5 wt%	12.10 ± 0.08	16.10 ± 0.12	220 ± 3	224 ± 2
5 wt%	13.20 ± 0.12	14.50 ± 0.30	222 ± 5	224 ± 2
6.5 wt%	12.80 ± 0.2	19.10 ± 0.16	203 ± 6	222 ± 5

Table 4
The values of loss peak height and nano hardness (H).

Sample	Parameter			
	Loss peak height		H (GPa)	
	Before exposure to electrolyte	After exposure to electrolyte	Before exposure to electrolyte	Before exposure to electrolyte
3.5 wt%	1.09 ± 0.05	1.12 ± 0.03	0.16 ± 0.02	0.14 ± 0.01
5 wt%	1.40 ± 0.12	1.25 ± 0.10	0.14 ± 0.01	0.13 ± 0.02
6.5 wt%	1.17 ± 0.09	1.15 ± 0.04	0.17 ± 0.01	0.15 ± 0.01

Fig. 1 shows that blank epoxy coating was severely deteriorated after 60 days immersion. Results can clearly show severe creation of blisters and corrosion products on this sample. These observations show that corrosive electrolyte severely diffused into the coating/metal interface. The severe hydrolytic degradation of the blank epoxy coating can be seen from the lots of holes and defects which were produced on the surface of this sample (Fig. 1-b). Increase in size and number of holes can occur at long immersion times.

The visual performance and morphology of the nanocomposites are shown in Fig. 2.

As it can be seen in Fig. 2, the number of defects and blisters were significantly reduced using nanoparticles. Moreover, lower corrosion products were produced in presence of nanoparticles. These observations reveal that nanoparticles can significantly improve coating resistance against hydrolytic degradation. The improvement was more pronounced at 3.5 and 5 wt%. However, decrease in corrosion resistance of the coating was observed at 6.5 wt%. This may be attributed to the nanoparticles aggregation at 6.5 wt% [33,34].

3.3. Investigation of the nano-ZnO/composite degradation

3.3.1. DMTA and nano-indentation measurements

Mechanical properties of the epoxy nanocomposites were investigated before and after exposure to corrosive electrolyte. Variations of tan Δ and storage modulus versus temperature of the blank sample are shown in Fig. 3. Moreover, variations of force versus displacement of this sample are also shown in Fig. 3. The values of cross-linking density (υ_e), loss peak height, loss peak width, hardness (H) and indentation depth (D_{max}) of the blank sample were calculated from DMTA and indentation curves (Table 2).

As it can be seen in Table 2, the mechanical properties of the blank epoxy coating were significantly affected after exposure to corrosive electrolyte. Results can show significant decrease in values of cross-linking density, loss peak width, loss peak depth and nano-hardness of the blank sample. Moreover, increase in indentation depth of the blank sample was observed after 60 days immersion. These results show that corrosive electrolyte can significantly influence the mechanical properties of the blank sample. Decrease in cross-linking density and hardness of the coating can be attributed to the significant hydrolytic degradation of this sample. Decrease in loss peak height and increase in indentation depth of the blank sample can also reveal poor damping behavior and
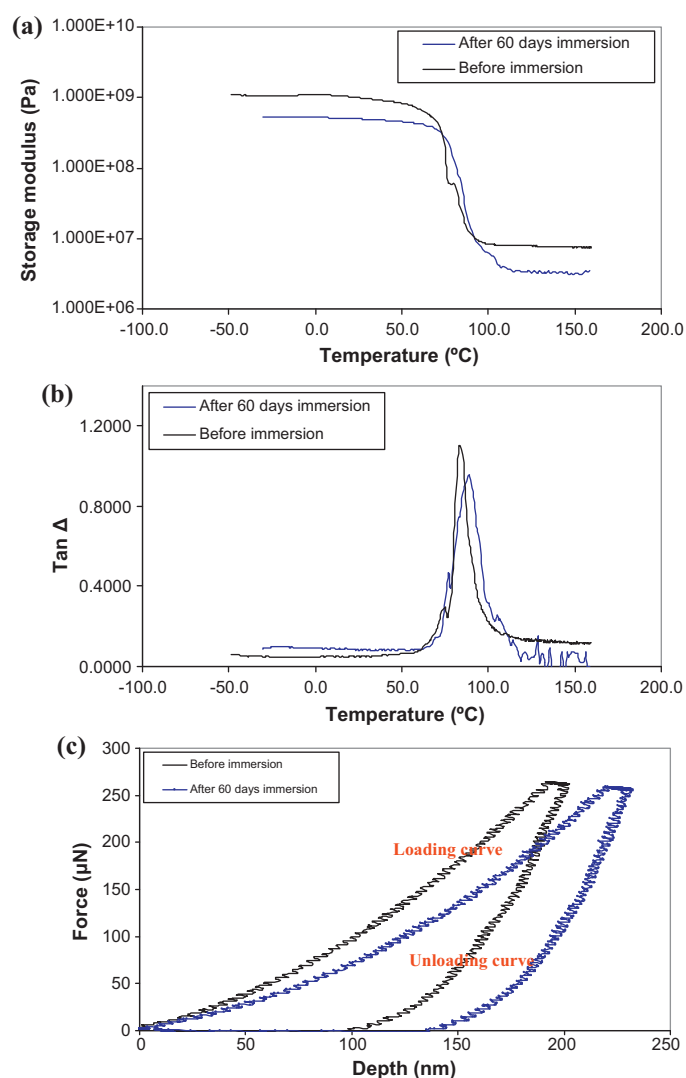

Fig. 3. Variations of (a) storage modulus versus temperature, (b) tan Δ versus temperature and (c) force versus displacement of the blank epoxy coating exposed to 3.5% NaCl solution.

poor mechanical properties of coating after exposure to corrosive electrolyte.

Variations of force versus displacement and storage modulus versus temperature of the nanocomposites are shown in Figs. 4 and 5.

The values of cross-linking density (υ_e), loss peak height, loss peak width, hardness (H) and indentation depth (D_{max}) of the nanocomposites were calculated from DMTA and indentation curves (Tables 3 and 4).

As it can be seen in Fig. 6, the cross-linking density of the epoxy coating was decreased using ZnO nanoparticles. Decrease in cross-linking density was more pronounced at 5 wt%. It has been shown that [33] ZnO nanoparticles can reduce curing degree of the epoxy coating. It has been also found that nanoparticles can produce strong physical interactions with coating matrix [33]. Decrease in

Table 5

The variations of Δ [NH/NH$_2$ and OH]/[CH] (normalized with respect to –CH bond) and Δ [etheric bonds] of the coatings exposed to 3.5 wt% NaCl solution; Δ (the hydroxyl or etheric frequency intensity after exposure – the hydroxyl or etheric frequency intensity before exposure).

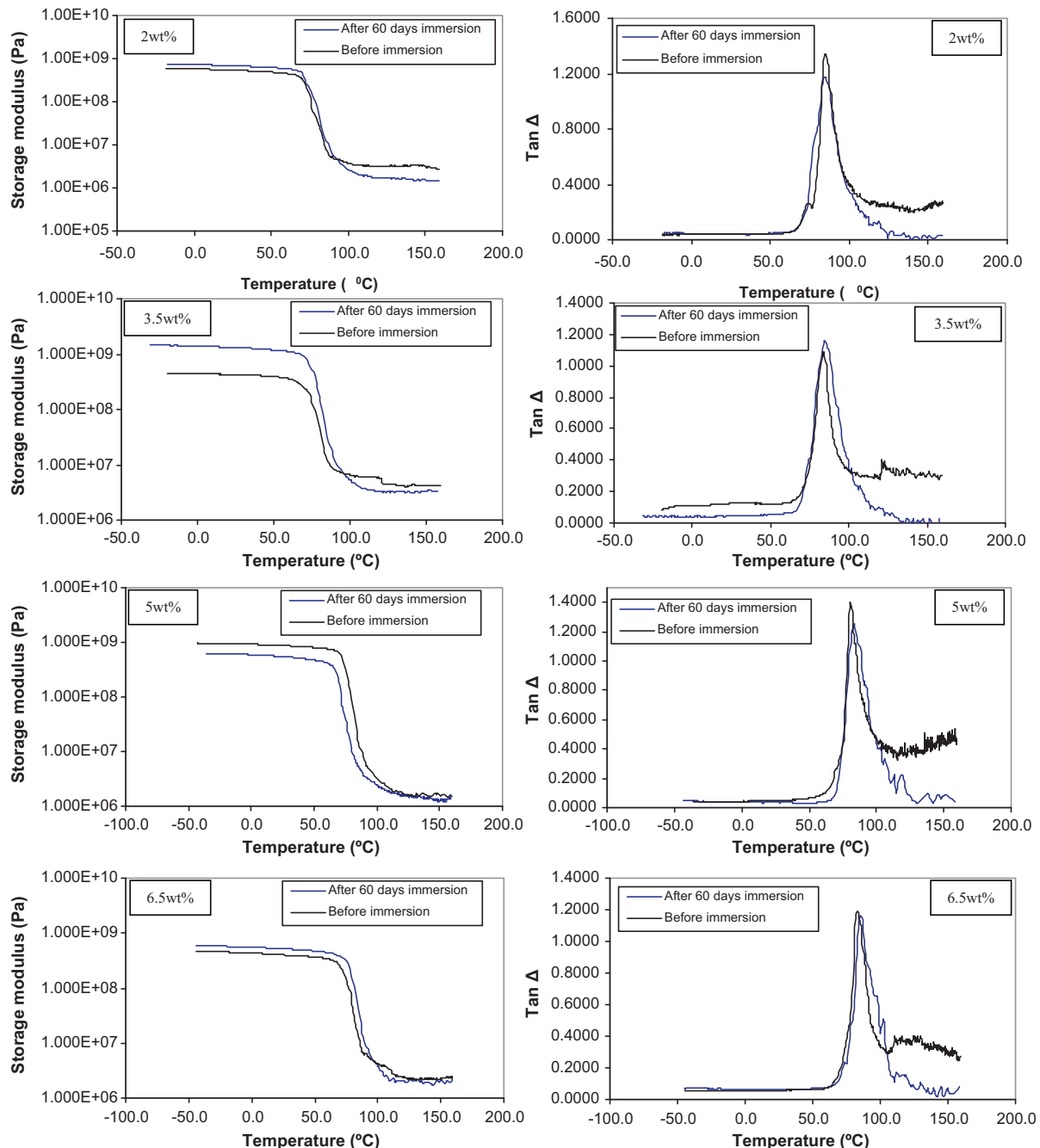| Sample	Parameter	
	Δ [NH/NH$_2$ and OH]/CH] (3400–3500 cm^{-1})	Δ [Etheric bonds] (1035 cm^{-1})
Blank sample	6.77 ± 0.65	−1.24 ± 0.20
2 wt%	4.83 ± 0.45	−0.92 ± 0.18
3.5 wt%	3.51 ± 0.12	−0.50 ± 0.15
5 wt%	3.00 ± 0.25	−0.46 ± 0.18
6.5 wt%	4.00 ± 0.33	−0.56 ± 0.12

Fig. 4. Variations of storage modulus versus temperature and tan Δ versus temperature of the nanocomposites exposed to 3.5% NaCl solution.
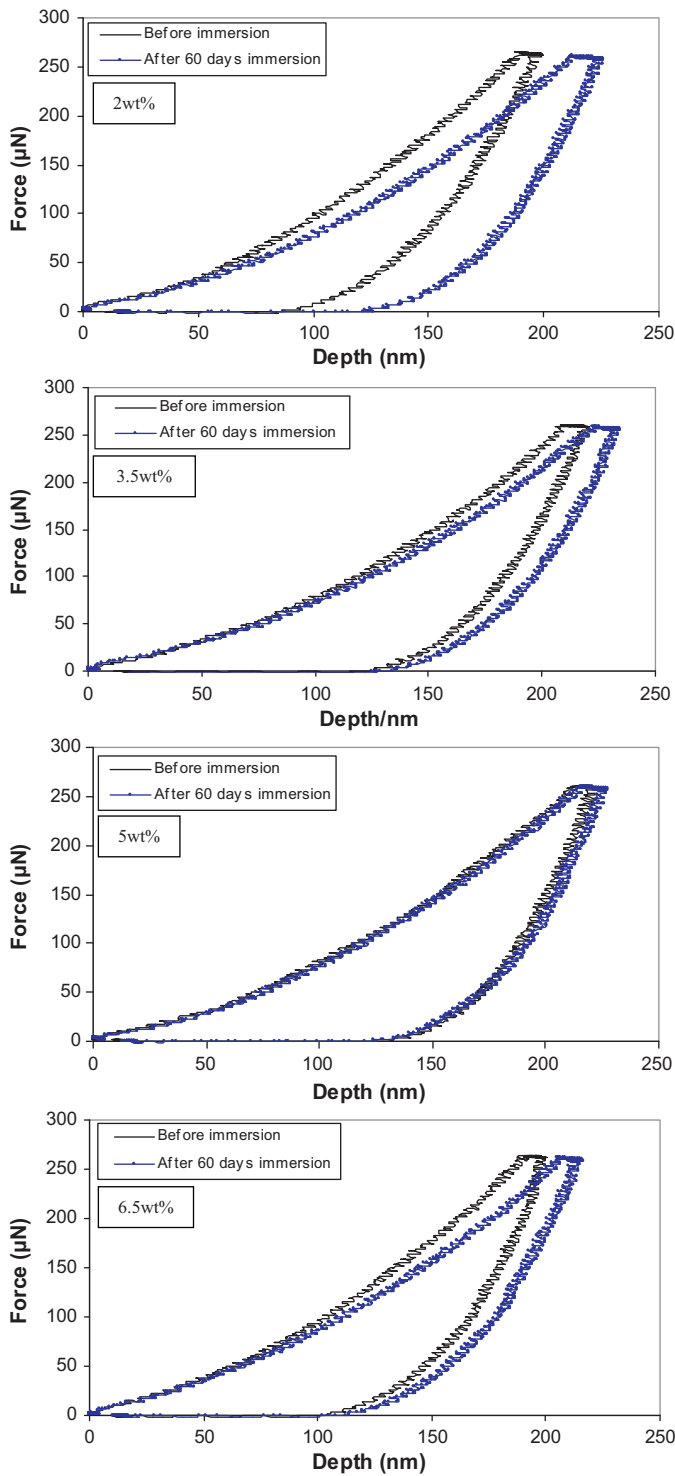
Fig. 5. Variations of force versus displacement of the nanocomposites exposed to 3.5% NaCl solution.

Fig. 6. The values of cross-linking density of the epoxy coatings containing different contents of ZnO nanoparticles (before and after exposure to 3.5% NaCl solution).

Fig. 7. FTIR spectrums of the blank epoxy coating exposed to 3.5 wt% NaCl solution.

Fig. 8. FTIR spectrums of the epoxy nanocomposites exposed to 3.5 wt% NaCl solution.

both cross-linking density and nano-hardness of the nanocomposites were observed after 60 days immersion. However, decrease in cross-linking density (and hardness) of the nanocomposites was significantly lower than blank sample. Moreover, increase in indentation depth of the blank epoxy coating was significantly higher than nanocomposites. Results show that nanoparticles can significantly increase coating resistance against hydrolytic degradation. Increase in coating resistance against hydrolytic degradation was more pronounced at 3.5 and 5 wt%.
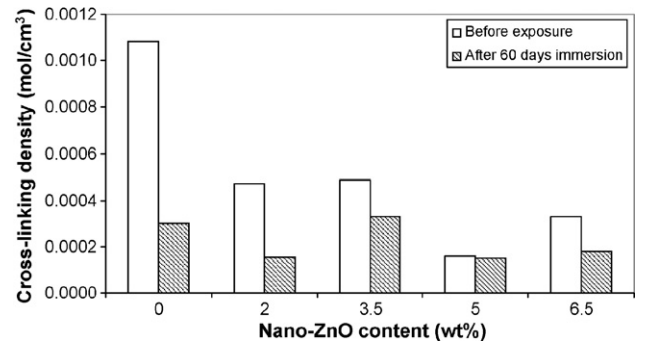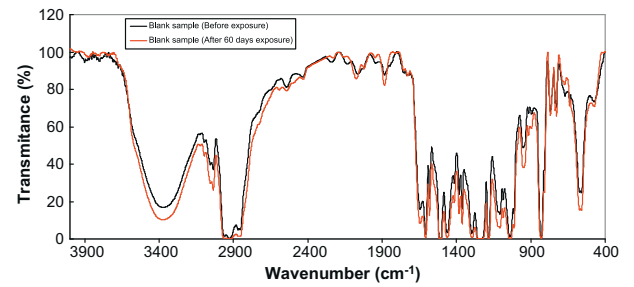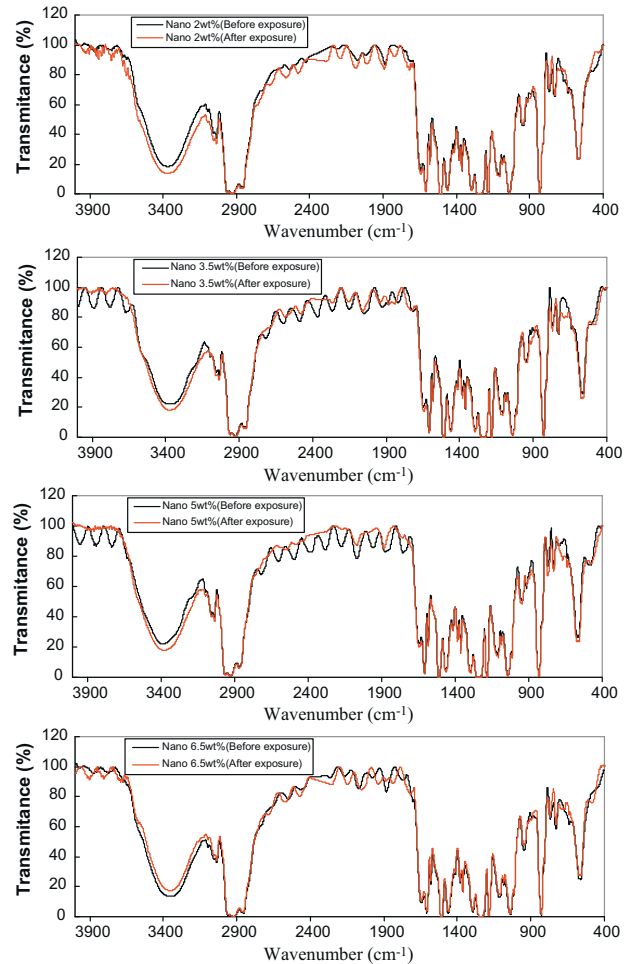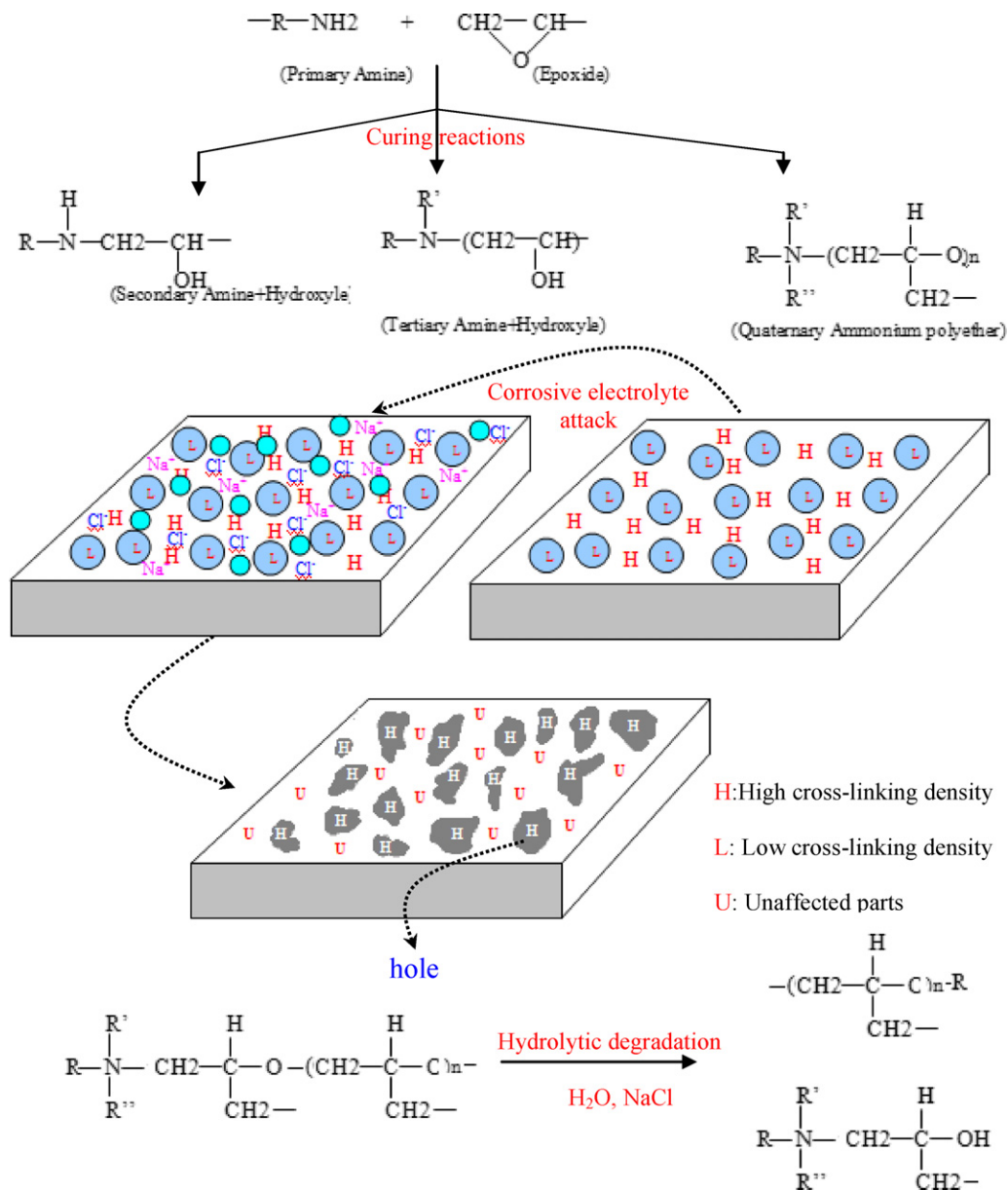
Fig. 9. Schematic illustration of the mechanism of hydrolytic degradation of an epoxy coating exposed to 3.5 wt% NaCl solution.

3.3.2. FTIR analysis

Hydrolytic degradation of the coatings exposed to corrosive electrolyte was studied by a FTIR technique. FTIR spectrums of the blank epoxy coating and nanocomposites are shown in Figs. 7 and 8.

Figs. 7 and 8 show a greater hydrolytic degradation of the blank epoxy coating than nanocopmposites. This can be understood from variations of hydroxyl (–OH) (3400–3500 cm^{-1}) and etheric (–C–O–C–) (1035 cm^{-1}) bonds intensities [33,35]. Variations of Δ [NH/NH$_2$ and OH]/[CH] (normalized with respect to –CH bond intensity) and Δ [etheric bonds] of the nanocomposites are shown in Table 5.

It is well known that hydrolytic degradation of an epoxy coating can lead to an increase in vibration bond intensity of OH (3400–3500 cm^{-1}) and a decrease in vibration bond intensity of etheric bonds (1035 cm^{-1}). As it can be seen in Table 5, the value of Δ [NH/NH$_2$ and OH]/[CH] was significantly reduced using nanoparticles. Decrease in value of Δ [NH/NH$_2$ and OH]/[CH] was more pronounced at 3.5 and 5 wt%. The value of Δ [etheric bonds] of the blank sample was more negative compared to

nanocopmosites. Variations of Δ [etheric bonds] of the composites reinforced with 3.5 and 5 wt% nanoparticles were significantly lower than blank sample. Therefore, higher values of Δ [NH/NH$_2$ and OH]/[CH] and Δ [etheric bonds] of the blank sample compared to nanocomposites can reveal greater hydrolytic degradation of this sample. These observations are completely in agreement with the results shown in Tables 3 and 4. The mechanism of hydrolytic degradation of an epoxy coating is schematically shown in Fig. 9.

Fig. 9 shows that epoxy coating contains etheric linkages (–C–O–C–). Etheric linkage is extremely sensitive to humid condition. Therefore, etheric bonds cleavage can occur during coating exposure to corrosive electrolyte. As it can be seen in Fig. 9, there are areas on the surface of coating which have lower cross-linking density than other parts. Coating degradation will be started from areas which have lower cross-linking density. Coating degradation can result in holes and defects creation on the surface of coating [36,37]. Increase in size and number of holes are expectable at long immersion times.

According to the above explanations, although, the cross-linking density of the nanocomposites was considerably lower than blank sample, the rate of hydrolytic degradation of the blank sample was higher than nanocomposites. These observations will be explained later.

3.4. EIS measurements

Corrosion resistance of the epoxy nanocomposites were studied by an EIS technique. The Nyquist and Bode plots of samples are shown in Figs. 10–12.

Two time constant semicircle was observed for the blank sample which was exposed to corrosive electrolyte up to 15 days. This means that corrosive electrolyte diffused into the coating/metal interface at very short immersion time. Corrosion resistance of the blank sample was evaluated using electrochemical model shown in Fig. 10. Using this model, the values of R_s (solution resistance), R_c (coating resistance), C_{dl} (double layer capacitance), C_c (coating capacitance) and R_{ct} (charge transfer resistance) of the blank sample were calculated. Unlike blank sample, one time constant semi-circle was observed for the coatings reinforced with 3.5, 5 and 6.5 wt% nanoparticles. This means that corrosive electrolyte did not diffuse into the coating/metal interface of these samples. Using electrical models shown in Figs. 11 and 12, the values of polarization resistance R_p (R_{ct} (charge transfer resistance) + R_c (coating resistance) of the samples were calculated.
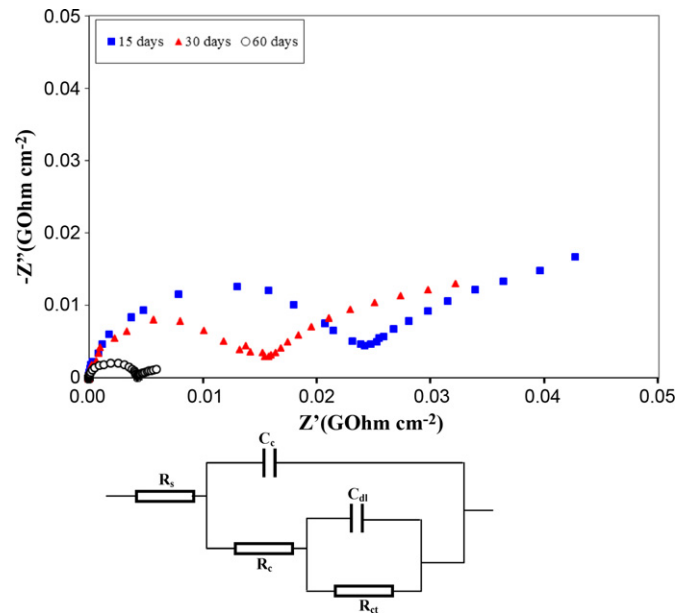

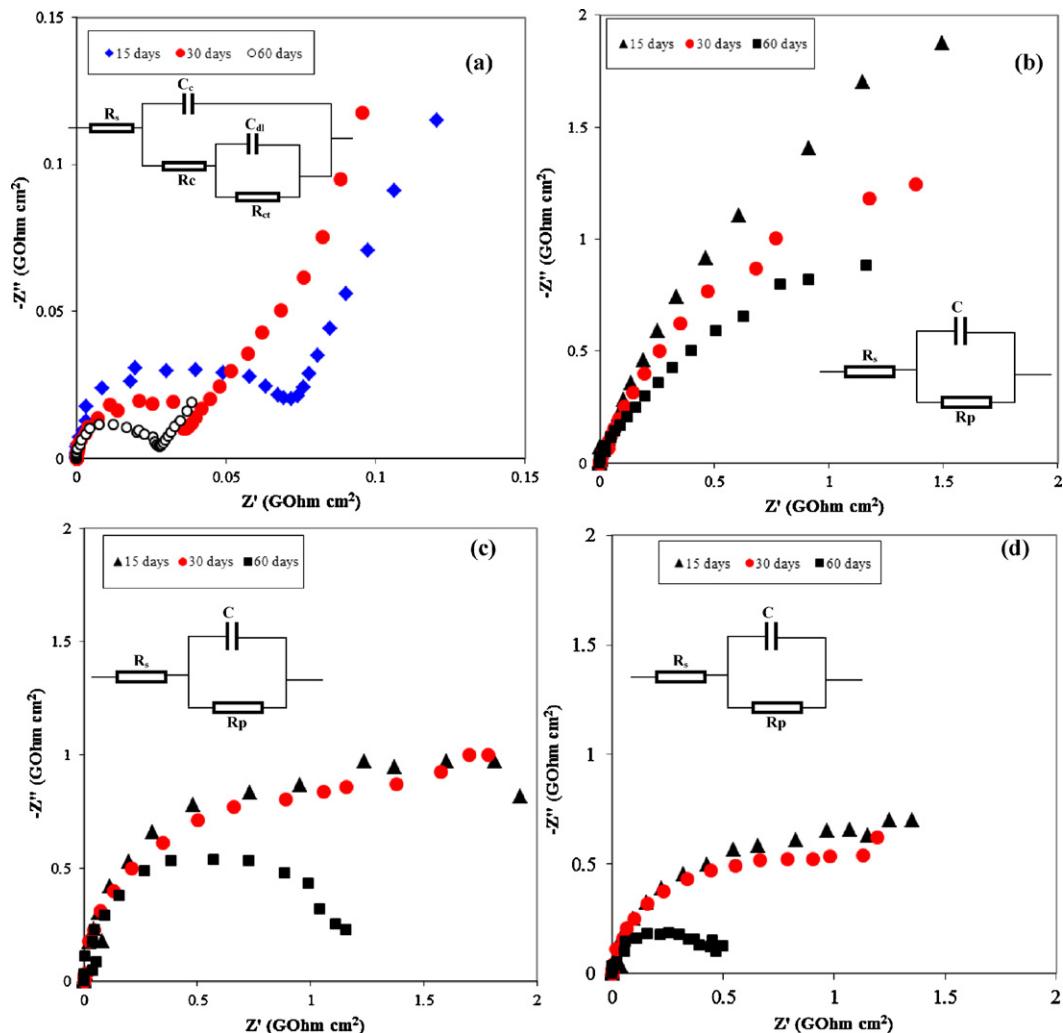**Fig. 10.** Nyquest plots of the blank epoxy coating exposed to 3.5 wt% NaCl solution up to 60 days.

Fig. 11. Nyquest plots of the nanocomposites reinforced with (a) 2 wt%, (b) 3.5 wt%, (c) 5 wt% and (d) 6.5 wt% nanoparticles exposed to 3.5 wt% NaCl solution.
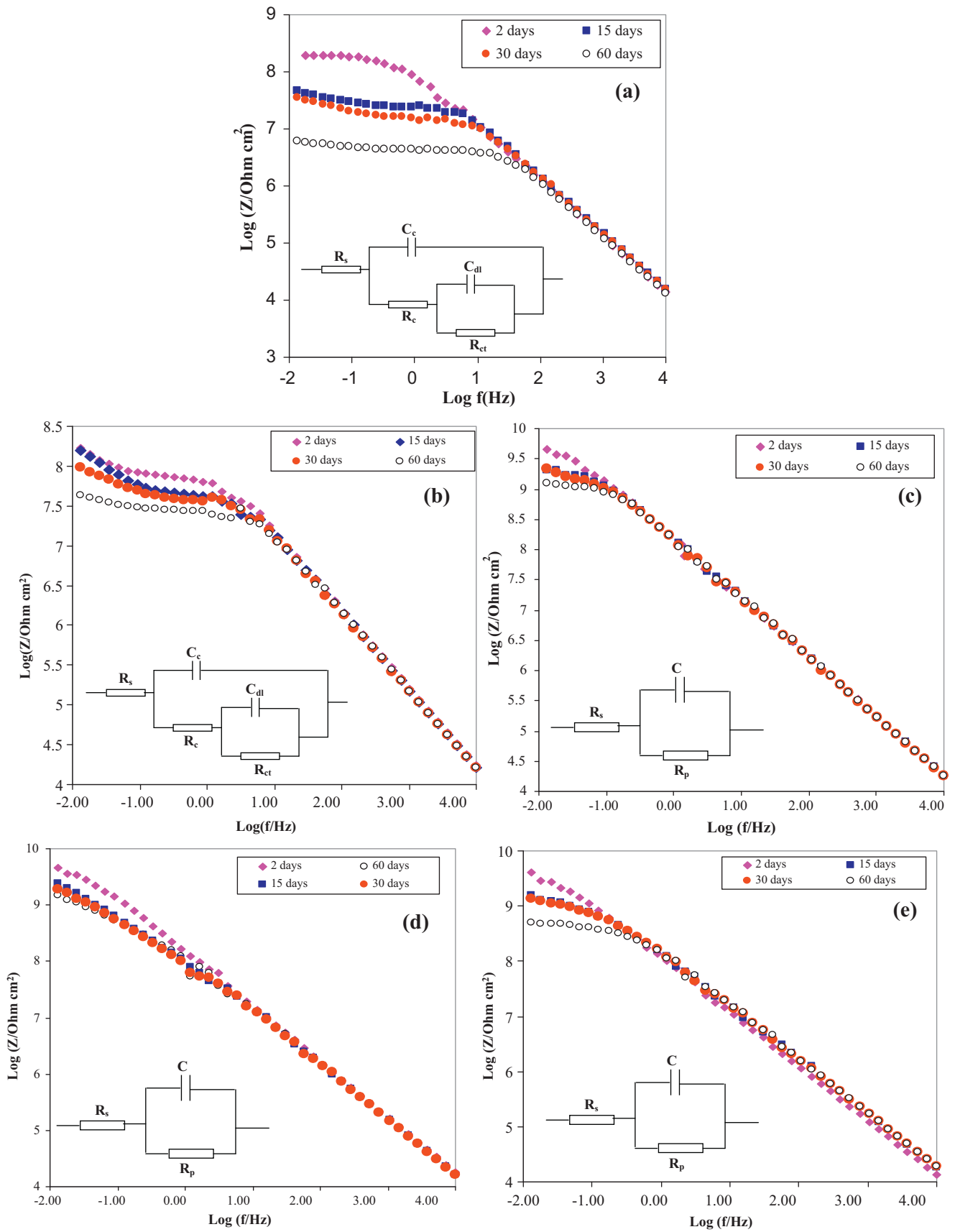
Fig. 12. Bode plots of the nanocomposites reinforced with (a) 0 wt%, (b) 2 wt%, (c) 3.5 wt%, (d) 5 wt% and (e) 6.5 wt% nanoparticles exposed to 3.5 wt% NaCl solution.

Table 6
The values of polarization resistance ($R_p = R_{ct}$ (charge transfer resistance) $+ R_c$ (Coating resistance)) and impedance at lowest frequency (10 mHz) of the samples exposed to 3.5 wt% NaCl solution at different immersion times.

Sample	Parameter							
	Log (Z/Ohm cm²) at 10 mHz				R_p (GOhm cm²)			
	Immersion times (days)				Immersion times (days)			
	2	15	30	60	2	15	30	60
Blank sample	8.222	7.661	7.54	6.782	0.18	0.024	0.015	0.00044
2 wt%	8.293	8.198	7.99	7.635	0.25	0.071	0.038	0.0290
3.5 wt%	9.664	9.380	9.321 9.164	4.80	2.66	2.26	1.86	
5 wt%	9.663	9.332	9.269	9.10	4.76	2.02	1.20	1.07
6.5 wt%	9.614	9.330	9.222	8.711	4.64	1.48	1.032	0.83
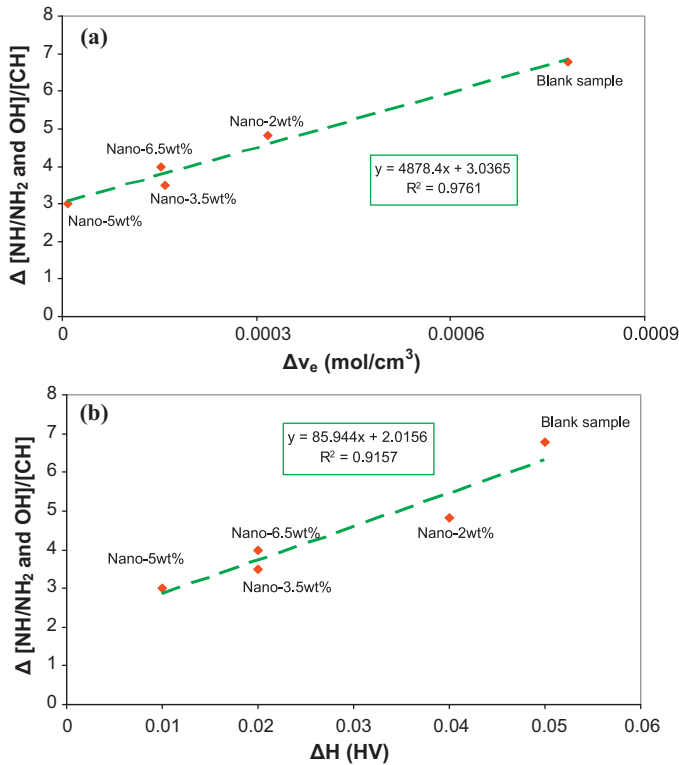
Fig. 13. The relationships between (a) Δ [NH/NH$_2$ and OH]/[CH] and Δv_e, and (b) Δ [NH/NH$_2$ and OH]/[CH] and ΔH.

Fig. 14. The relationships between (a) impedance (at 10 mHz) and ΔH, and (b) impedance (at 10 mHz) and Δ [NH/NH$_2$ and OH]/[CH].

The values of polarization resistance (R_p ($R_{ct} + R_c$)) and impedance at lowest frequency (10 mHz) of different samples are shown in Table 6. It is well known that impedance at lowest frequency (in Bode plots) can show total effects of first and second semi-circles in Nyquist plots on coating resistance against corrosion.

As it can be seen in Table 6, the R_p and impedance (10 mHz) of the blank epoxy coating were significantly decreased after 15 days immersion. This can reveal significant electrolyte diffusion into the coating matrix. Increase in R_p and impedance (at 10 mHz) of the coating were obtained using nanoparticles. Increase in R_p and impedance were more pronounced at 3.5 and 5 wt%. Two main reasons can be responsible for the higher corrosion resistance of nanocomposites compared to blank sample. First, ZnO nanoparticles could significantly increase the barrier properties of coating. Second, nanoparticles can significantly improve coating resistance against hydrolytic degradation. Decrease in R_p and impedance of coatings were observed at long immersion times. However, decrease in corrosion resistance of blank sample was higher than nanocomposites. Decrease in corrosion resistance was observed at nanoparticle loading greater than 5 wt%. This can be
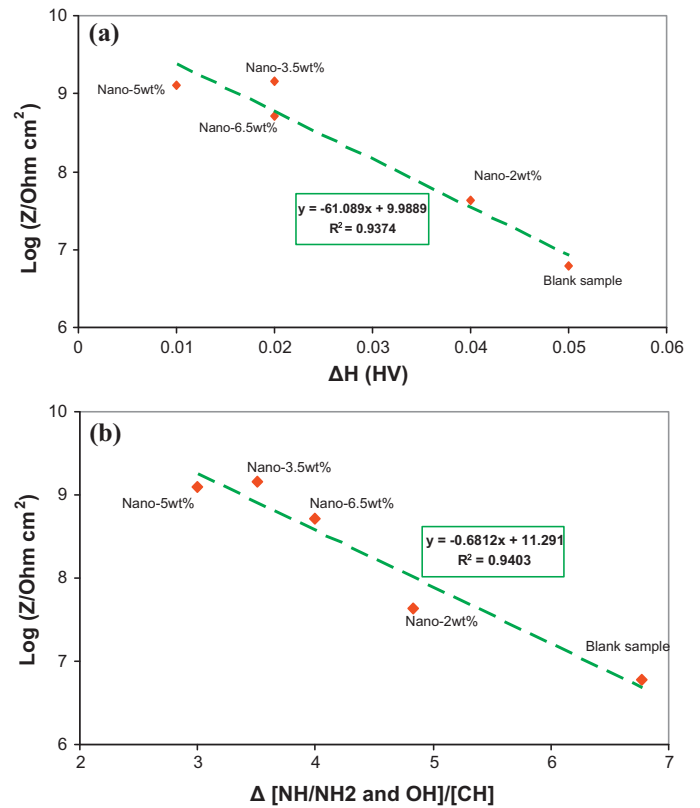
attributed to decrease in barrier properties of coating due to particles aggregation [33].

According to the above explanations, nanoparticles can significantly improve coating resistance against corrosion and hydrolytic degradation.

The relationships between different parameters are shown in Figs. 13 and 14.

Fig. 13 shows that the relationship between Δ [NH/NH$_2$ and OH]/[CH] and ΔH is linear. Moreover, the relationship between Δ [NH/NH$_2$ and OH]/[CH] and Δv_e is also linear. Results show that increase in Δ [NH/NH$_2$ and OH]/[CH] caused decrease in Δv_e and ΔH. These results show that coating degradation (increase in Δ [NH/NH$_2$ and OH]/[CH]) is responsible for decrease in hardness and cross-linking density of the coating exposed to corrosive electrolyte. Results can also show that increase in nanoparticles loading can reduce Δv_e and ΔH by decreasing Δ [NH/NH$_2$ and OH]/[CH].

Fig. 14 shows that the relationship between impedance and Δ [NH/NH$_2$ and OH]/[CH] is linear. A linear relationship between impedance and ΔH can be also seen in Fig. 14. Fig. 14 shows
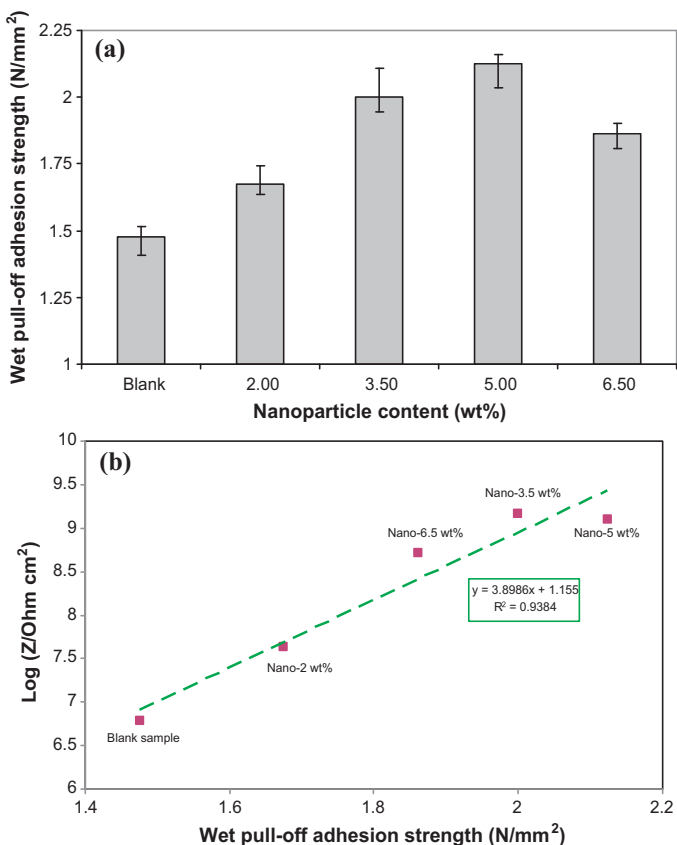
Fig. 15. (a) Wet pull-off adhesion strength of the nanocomposites exposed to 3.5 wt% NaCl solution up to 60 days and (b) the relationship between corrosion resistance and wet pull-off adhesion strength of the nanocomposites.

that increase in Δ [NH/NH$_2$ and OH]/[CH] and ΔH led to decrease in impedance. Nanoparticles can increase impedance by decreasing Δ [NH/NH$_2$ and OH]/[CH] and ΔH. It seems that increase in nanoparticles loading up to 5 wt% can cause decrease in hydrolytic degradation (and therefore increase in corrosion resistance) of the coating.

3.5. Adhesion measurements

The corrosive electrolyte diffusion into the coating/metal interface may lead to a decrease in adhesion of coating to metal substrate. It has been shown that the relationship between dry adhesion and corrosion resistance of an organic coating is not necessarily straightforward [5–8]. In addition, dry adhesion (compared to wet adhesion) is not an appropriate parameter to predict anticorrosion properties of an organic coating [5,6]. The wet pull-off adhesion strengths of the nanocomposites were measured after 60 days immersion (Fig. 15-a). The relationship between wet adhesion and impedance is shown in Fig. 15-b.

Fig. 15-a shows that increase in nanoparticles loading led to increase in wet pull-off adhesion strength. The lowest value of adhesion strength was observed on the blank sample. Moreover, increase in wet pull-off adhesion strength was more pronounced at 5 wt%. As it can be seen in Fig. 15-b, the relationship between wet pull-off adhesion and impedance is linear. This means that increase in impedance led to increase in wet adhesion strength. Results show that nanoparticles can increase wet adhesion by decreasing corrosion resistance of the coating. Nanoparticles can reduce electrolyte diffusion into the coating/metal interface. It is well known that when the electrolyte reaches to the coating/metal interface, the hydrolysis of adhesion bonds (which attach coating to metal

substrate) can be responsible for decrease in adhesion strength. Corrosion products creation beneath coating can be also responsible for decrease in coating adhesion. These mean that nanoparticles can reduce adhesion loss of coating by increasing coating resistance against electrolyte diffusion.

4. Conclusions

The effects of nano sized ZnO particles on the corrosion resistance and hydrolytic degradation of an epoxy coating were studied. The results obtained in this study are listed below:

- Results showed that cross-linking density of the epoxy coating was decreased in presence of nanoparticles. Nanoparticles can also increase physical interactions between particles and coating matrix.
- The cross-linking density and hardness of the blank sample was significantly decreased after exposure to corrosive electrolyte. The corrosion resistance of the blank sample was significantly decreased at short immersion time.
- ZnO nanoparticles increased coating resistance against hydrolytic degradation significantly. The cross-linking density and hardness of coating were decreased after exposure to corrosive electrolyte. Decrease in cross-linking density and hardness of the nanocomposites were higher than blank sample. It was found that nanoparticles can significantly increase corrosion resistance of the epoxy coating. Increase in corrosion resistance was more pronounced at 3.5 wt%.
- Decrease in wet adhesion strength of the blank epoxy coating was severer than nanocomposites. Nanoparticles can reduce adhesion loss of the coating.

References

[1] G. Bierwagen, D. Tallman, J. Li, L. He, C. Jeffcoate, EIS studies of coated metals in accelerated exposure, Prog. Org. Coat. 46 (2003) 148–157.
[2] C.G. Oliveira, M.G.S. Ferreira, Ranking high-quality paint systems using EIS. Part I: intact coatings, Corros. Sci. 45 (2003) 123–138.
[3] M.W. Wittmann, R.B. Leggat, S.R. Taylor, The detection and mapping of defects in organic coatings using local electrochemical impedance methods, J. Electrochem. 146 (11) (1999) 4071–4075.
[4] V.B. Miskovic-Stankovic, M.R. Stanic, D.M. Drazic, Corrosion protection of aluminium by a cataphoretic epoxy coating, Prog. Org. Coat. 36 (1999) 53–63.
[5] J.B. Bajat, V.B. Mišković-Stanković, N. Bibić, D.M. Dražić, Prog. Org. Coat. 58 (2007) 323.
[6] J.B. Bajat, V.B. Mišković-Stanković, J.P. Popić, D.M. Dražić, Prog. Org. Coat. 63 (2) (2008) 201.
[7] S. Palraj, M. Selvaraj, P. Jayakrishnan, Prog. Org. Coat. 54 (2005) 5.
[8] R.M. Souto, D.J. Scantlebury, Prog. Org. Coat. 53 (2005) 63.
[9] H.L. Yang, F.C. Lin, E.H. Han, Effects of P/B on the properties of anticorrosive coatings with different particle size, Prog. Org. Coat. 53 (2005) 91–98.
[10] S.K. Dhoke, A.S. Khanna, Electrochemical behavior of nano-iron oxide modified alkyd based waterborne coatings, Mater. Chem. Phys. 117 (2009) 550–556.
[11] H. Yari, S. Moradian, B. Ramazanzade, A. Kashani, N. Tahmasebi, The effect of basecoat pigmentation on mechanical properties of an automotive basecoat/clearcoat system during weathering, Polym. Deg. Stab. 94 (8) (2009) 1281–1289.
[12] F.X. Perrin, M. Irigoyen, E. Aragon, J.L. Vernet, Evaluation of accelerated weathering tests for three paint systems: a comparative study of their aging behaviour, Polym. Deg. Stab. 72 (1) (2001) 115–124.
[13] T. Nguyen, J.W. Martin, E. Byrd, N. Embree, Relating laboratory and outdoor exposure of coatings III. Effect of relative humidity on moisture-enhanced photolysis of acrylic-melamine coatings, Polym. Deg. Stab. 77 (2002) 1–16.
[14] J.W. Martin, T. Nguyen, E. Byrd, B. Dickens, N. Embree, Relating laboratory and outdoor exposures of acrylic melamine coatings I. Cumulative damage model and laboratory exposure apparatus, Polym. Deg. Stab. 75 (2002) 193–210.
[15] M. Mahdavian, M.M. Attar, Another approach in analysis of paint coatings with EIS measurement: phase angle at high frequencies, Corros. Sci. 48 (12) (2006) 4152–4157.
[16] F. Mansfeld, L.T. Han, C.C. Lee, G. Zhang, Evaluation of corrosion protection by polymer coatings using electrochemical impedance spectroscopy and noise analysis, Electrochim. Acta 43 (1998) 2933–2945.
[17] M. Hu, J.Q. Zhang, C.N. Cao, Determination of water uptake and diffusion of Cl⁻ ion in epoxy primer on aluminum alloys in NaCl solution by electrochemical impedance spectroscopy, Prog. Org. Coat. 46 (2003) 273–279.

[18] C.G. Oliveira, M.G.S. Ferreira, Ranking high-quality paint systems using EIS. Part II: defective coatings, Corros. Sci. 45 (2003) 139–147.

[19] M. Mierisch, S.R. Taylor, Understanding the degradation of organic coatings using local electrochemical impedance methods – I. Commonly observed features, J. Electrochem. 150 (7) (2003) B303–B308.

[20] V.B. Miskovic-Stankovic, D.M. Drazic, M.J. Teodorovic, Electrolyte penetration through epoxy coatings electrodeposited on steel, Corros. Sci. 37 (1995) 241–252.

[21] V.B. Miskovic-Stankovic, D.M. Drazic, Z. Kacarevic-Popovic, The sorption characteristics of epoxy coatings electrodeposited on steel during exposure to different corrosive agents, Corros. Sci. 38 (1996) 1513–1523.

[22] V.B. Miskovic-Stankovic, M.D. Maksimovic, Z. Kacarevic-Popovic, J.B. Zotovic, The sorption characteristics and thermal stability of epoxy coatings electrodeposited on steel and steel electrochemically modified by Fe–P alloys, Prog. Org. Coat. 33 (1998) 68–75.

[23] M. Szociński, K. Darowicki, K. Schaefer, Identification and localization of organic coating degradation onset by impedance imaging, Polym. Deg. Stab. 95 (6) (2010) 960–964.

[24] E.P.M. Van Westing, G.M. Ferrari, J.H.W. De Wit, The determination of coating performance with impedance measurements – II. Water uptake of coatings, Corros. Sci. 36 (1994) 957–977.

[25] F. Deflorian, L. Fedrizzi, S. Rossi, P.L. Bonora, Organic coating capacitance measurement by EIS: ideal and actual trends, Electrochim. Acta 44 (1999) 4243–4249.

[26] R. Naderi, M.M. Attar, Electrochemical study of protective behavior of organic coating pigmented with zinc aluminum polyphosphate as a modified zinc phosphate at different pigment volume concentrations, Prog. Org. Coat. 66 (3) (2009) 314–320.

[27] R. Naderi, M.M. Attar, The role of zinc aluminum phosphate anticorrosive pigment in protective performance and cathodic disbondment of epoxy coating, Corros. Sci. 52 (2010) 1291–1296.

[28] X. Zhang, F. Wang, Yuanlong Du, Effect of nano-sized titanium powder addition on corrosion performance of epoxy coatings, Surf. Coat. Technol. 201 (2007) 7241–7245.

[29] S.K. Dhoke, A.S. Khanna, T. Jai Mangal Sinha, Effect of nano-ZnO particles on the corrosion behavior of alkyd-based waterborne coatings, Prog. Org. Coat. 64 (2009) 371–382.

[30] S.K. Dhoke, A.S. Khanna, Effect of nano-Fe_2O_3 particles on the corrosion behavior of alkyd based waterborne coatings, Corros. Sci. 51 (2009) 6–20.

[31] H. Shi, F. Liu, E. Han, Y. Wei, Effects of nano pigments on the corrosion resistance of alkyd coatings, J. Mater. Sci. Technol. 23 (4) (2007) 551–558.

[32] S.K. Dhoke, A.S. Khanna, Study on electrochemical behavior of nano-ZnO modified alkyd-based waterborne coatings, J. Appl. Polym. Sci. 113 (2009) 2232–2237.

[33] B. Ramezanzadeh, M.M. Attar, M. Farzam, Effect of ZnO nanoparticles on the thermal and mechanical properties of epoxy-based, nanocomposite, J. Therm. Anal. Calorim. 103 (2010) 731–739.

[34] B. Ramezanzadeh, M.M. Attar, Characterization of the fracture behavior and viscoelastic properties of epoxy-polyamide coating reinforced with nanometer and micrometer sized ZnO particles, Prog. Org. Coat. 11 (2011) 242–249.

[35] G. Nikolic, S. Zlatkovic, M. Cakic, S. Cakic, C. Lacnjevac, Z. Rajic, Fast fourier transform IR characterization of epoxy GY systems crosslinked with aliphatic and cycloaliphatic EH polyamine adducts, Sensors (2010), doi:10.3390/s100100684.

[36] S. Sangaj, V.C. Malshe, Permeability of polymers in protective organic coatings, Prog. Org. Coat. 50 (2004) 28–39.

[37] T. Nguyen, J. Martin, E. Byrd, N. Embree, Relating laboratory and outdoor exposure of coatings II. Effects of relative humidity on photodegradation and the apparent quantum yield of acrylic melamine coatings, J. Coat. Technol. 74 (932) (2002) 65–80.